Journal of Proteomics 154 (2017) 1–12

Contents lists available at ScienceDirect

Journal of Proteomics

journal homepage: www.elsevier.com/locate/jprot

Malonylome analysis of rhizobacterium *Bacillus amyloliquefaciens* FZB42 reveals involvement of lysine malonylation in polyketide synthesis and plant-bacteria interactions

Ben Fan [a], Yu-Long Li [a], Lei Li [b], Xiao-Jun Peng [c], Chen Bu [c], Xiao-Qin Wu [a,*], Rainer Borriss [d,*]

[a] Co-Innovation Center for Sustainable Forestry in Southern China, College of Forestry, Nanjing Forestry University, 210037 Nanjing, China
[b] RNA Biology Group, Institute for Molecular Infection Biology, University of Würzburg, 97080 Würzburg, Germany
[c] Jingjie PTM Biolabs (Hangzhou) Co. Ltd., Hangzhou 310018, China
[d] Fachgebiet Phytomedizin, Albrecht Daniel Thaer Institut für Agrar- und Gartenbauwissenschaften, Lebenswissenschaftliche Fakultät, Humboldt Universität zu Berlin, 14195 Berlin, Germany

ARTICLE INFO

Article history:
Received 28 September 2016
Received in revised form 24 November 2016
Accepted 30 November 2016
Available online 08 December 2016

Keywords:
Malonylome
Malonylation
Bacillus amyloliquefaciens
FZB42
Polyketide synthetase
Plant-microbe interaction

ABSTRACT

Using the combination of affinity enrichment and high-resolution LC-MS/MS analysis, we performed a large-scale lysine malonylation analysis in the model representative of Gram-positive plant growth-promoting rhizobacteria (PGPR), *Bacillus amyloliquefaciens* FZB42. Altogether, 809 malonyllysine sites in 382 proteins were identified. The bioinformatic analysis revealed that lysine malonylation occurs on the proteins involved in a variety of biological functions including central carbon metabolism, fatty acid biosynthesis and metabolism, NAD(P) binding and translation machinery. A group of proteins known to be implicated in rhizobacterium-plant interaction were also malonylated; especially, the enzymes responsible for antibiotic production including polyketide synthases (PKSs) and nonribosomal peptide synthases (NRPSs) were highly malonylated. Furthermore, our analysis showed malonylation occurred on proteins structure with higher surface accessibility and appeared to be conserved in many bacteria but not in archaea. The results provide us valuable insights into the potential roles of lysine malonylation in governing bacterial metabolism and cellular processes.

Biological significance: Although in mammalian cells some important findings have been discovered that protein malonylation is related to basic metabolism and chronic disease, few studies have been performed on prokaryotic malonylome. In this study, we determined the malonylation profiles of *Bacillus amyloliquefaciens* FZB42, a model organism of Gram-positive plant growth-promoting rhizobacteria. FZB42 is known for the extensive investigations on its strong ability of producing antimicrobial polyketides and its potent activities of stimulating plant growth. Our analysis shows that malonylation is highly related to the polyketide synthases and the proteins involved bacterial interactions with plants. The results not only provide one of the first malonylomes for exploring the biochemical nature of bacterial proteins, but also shed light on the better understanding of bacterial antibiotic biosynthesis and plant-microbe interaction.

1. Introduction

Rhizobacteria are a group of heterogenic bacteria living in the vicinity of plant roots. Most rhizobacteria are beneficial to plants via a series of known mechanisms. For example, rhizobacteria can i) provide nutrient substrates to plants by mineralization of soil minerals and complex organic compounds, ii) induce plant systemic resistance to stress environments, and iii) promote plant growth by secreting phytohormones like indole-3-acetic acid (IAA) or gibberellic acid [1]. Also importantly, many rhizobacteria protect host plants from soil-borne phytopathogens by synthesizing a variety of antibiotics [2], or by forming robust biofilms, a physical barrier on plant roots against pathogens. Many competent rhizobacterial strains have been used to develop biofertilizer or biocontrol agents.

Two important groups of rhizobacterial antibiotics are nonribosomally synthesized polyketides and lipopeptides, which are produced from the precursors derived from primary metabolism [2,3]. Biosynthesis of these antibiotics is rather energy costing and controlled by a dynamic complex regulatory network [4]. Thus, to unveil the regulatory mechanism and to promote biosynthesis of these antimicrobial metabolites is a promising direction for the formulation of better microbial fertilizers or even clinic agents.

The regulation of bacterial gene expression can be controlled at several levels including post-translational modifications (PTM), e.g. protein

* Corresponding authors.
E-mail addresses: fanben2000@gmail.com (B. Fan), lyj.lylo@163.com (Y.-L. Li), lei.li1@uni-wuerzburg.de (L. Li), xiaojun_peng@ptm-biolab.com (X.-J. Peng), chen_bu@ptm-biolab.com (C. Bu), xqwu2015@gmail.com (X.-Q. Wu), rainer.borriss@rz.hu-berlin.de (R. Borriss).

http://dx.doi.org/10.1016/j.jprot.2016.11.022
1874-3919/

phosphorylation and ubiquitination. In recent years other PTM types such as acetylation, methylation, succinylation, crotonylation, and malonylation have been increasingly identified, benefiting from the progress of high-resolution mass spectrometry and improved purification methods [5–9]. PTM is ubiquitous in diverse organisms and known to play important roles in many cellular processes [10]. For example, lysine acetylation has been related with enzyme activity, protein localization and their interaction with other proteins or nucleic acids [7, 11]. Acetylation is not only prevalent in the enzymes for the primary metabolisms like glycolysis and citrate cycle [12,13], but also involved in secondary metabolism [14].

Although mostly carried out in eukaryotic cells, the studies of PTM have also been performed in many prokaryotes. For example, protein acetylation has been investigated in Gram-negative bacteria like *Escherichia coli* [15–20], *Salmonella enterica* [21–23], *Erwinia amylovora* [24], and *Thermus thermophiles* [25], and Gram-positive bacteria such as *Bacillus subtilis* [26], *Geobacillus kaustophilus* [27], *Streptomyces roseosporus* [14] and *B. amyloliquefaciens* subsp. *amyloliquefaciens* DSM7 [28]. The succinylomes have been characterized in *E. coli* [29, 30], *B. subtilis* [31,32], and *Mycobacterium tuberculosis* [33]. In recent years, malonylation is also drawing increasing attention [34–36]. For instance, the research on mammalian malonylome has highlighted the importance of lysine malonylation in type 2 diabetes and glycolysis [35,36]; the largest malonylome dataset so far revealed that lysine malonylation could contribute to pathophysiology of malonic aciduria and be associated with genetic disease [37]. However, until now only two prokaryotic malonylome has recently been characterized [38,39].

The strain *B. amyloliquefaciens* FZB42 is a representative of Gram-positive beneficial rhizobacteria, which has been extensively studied, particularly in its antagonism mechanisms against plant pathogens [2]. FZB42 is a potent antibiotic producer, able to synthesize ten antibiotic compounds including several non-ribosomally synthesized lipopeptides and three polyketides: bacillaene, difficidin, and macrolactin. These antibiotic compounds have been established to be efficient in control of fire blight disease, pathogenic nematodes, polluting algae, and bacterial leaf streak of rice [40–43]. The biosynthesis pathways of the polyketides have been elucidated previously [2,44–47].

It's conventionally known that lysine acetyltransferase (KAT) catalyzes the transfer of the acetyl group from acetyl-CoA to a lysine. Malonyl-CoA has been proposed to be the donor of malonylation [34]. Given that malonyl-CoA is indispensable for the polyketide biosynthesis, we were curious to know whether protein malonylation is occurring in FZB42 and whether it is linked with the biosynthesis of these polyketides. In this study, we exploited immunoaffinity enrichment strategies and mass spectrometry-based technologies to determine the malonylation profiles of *B. amyloliquefaciens* FZB42.

2. Material and methods

1. Bacterial strains and growth conditions

For assessment of the overall malonylation degree, *B. amyloliquefaciens* FZB42 was grown in chemically defined M9 medium (2 mM $MgSO_4$, 0.1 mM $CaCl_2$, 0.4% glucose,), routine Luria Broth (1% peptone, 0.5% yeast extract, 0.5% NaCl) and SE medium (1% peptone, 0.05% yeast extract, 0.5% NaCl, 10% soil extract) [48,49]. The cultures were incubated at 210 rpm and 37 °C. Optical density of the cultures was monitored at 600 nm. For protein preparation from biofilm, FZB42 was grown in static liquid Luria Broth at 30 °C and after 36 h the pellicle was picked out.

2. Western blotting

The extracted proteins were adjusted to be at the concentration of 2 mg/ml and then boiled in SDS loading buffer for 10 min. Then they were subjected to 12% SDS-PAGE and transferred to a polyvinylidene difluoride (PVDF) membrane. The membrane was blocked overnight at 37 °C for 2 h in TBS buffer (25 mM Tris-HCl, pH 8.0, 150 mM NaCl) containing 5% bovine serum albumin (BSA) and incubated with either the anti-succinyl lysine antibody (PTM Biolabs Inc., Hangzhou, China) (1:1000, in TBS/2.5% BSA) or the anti-malonyl lysine antibody (PTM Biolabs Inc., Hangzhou, China) (1:5000, in TBS/2.5% BSA) overnight at 4 °C. After washing three times with TBST buffer (25 mM Tris-HCl, pH 8.0, 150 mM NaCl, 0.1% Tween20), the membrane was incubated with horseradish peroxidase-conjugated goat anti-rabbit antibody (1:5000 dilutions) for 1 h at 37 °C. The membrane was then washed with TBST buffer and visualized with chemiluminescent HPR substrate (Immobilon™ Western, Millipore, USA). Finally, the blot was imaged with X-ray film (XBT, Carestream, Xiamen, China) at adequate exposure time.

3. Protein extraction

Three bacterial cultures of equal amount were pooled and then centrifuged for pellets before being grounded with liquid nitrogen. The cell powder was transferred to 5 ml centrifuge tube and sonicated three times on ice using a high intensity ultrasonic processor (Scientz, Ningbo, China) in lysis buffer (8 M urea, 10 mM dithiothreitol, 2 mM EDTA, 3 μM Trichostatin A, 50 mM Nicotinamide and 1% Protease Inhibitor Cocktail III). The remaining debris was removed by centrifugation at 20,000 g at 4 °C for 10 min. Finally, the protein was precipitated with cold 15% trichloroacetic acid for 2 h at −20 °C. After centrifugation at 4 °C for 10 min, the supernatant was discarded. The remaining precipitate was washed with cold acetone for three times. The protein was redissolved in buffer (8 M urea, 100 mM NH_4CO_3, pH 8.0) and the protein concentration was determined with 2-D Quant kit (GE Healthcare, USA) according to the manufacturer's instructions.

4. Trypsin digestion

For digestion, the protein solution was reduced with 10 mM dithiothreitol for 1 h at 37 °C and alkylated with 20 mM iodoacetamide for 45 min at room temperature in darkness. For trypsin digestion, the protein samples were diluted by adding 100 mM NH_4CO_3 till the concentration of urea in the samples was <2 M. Finally, trypsin was added at 1:50 trypsin-to-protein mass ratio for the first digestion overnight and 1:100 trypsin-to-protein mass ratio for a second 4 h-digestion. A total of 15 mg proteins were used for trypsin digestions. 300 μg and 150 μg trypsin were used for the first and the second step of digestion, respectively.

5. HPLC fractionation

The sample was fractionated by high pH reverse-phase HPLC using Agilent 300 Extend C18 column (5 μm particles, 4.6 mm ID, 250 mm length; Agilent Technologies, USA). Briefly, peptides were first separated with a gradient of 2% to 60% acetonitrile in 10 mM ammonium bicarbonate pH 10 over 80 min into 80 fractions, Then, the peptides were combined into 8 fractions and dried by vacuum centrifuging.

6. Affinity enrichment

To enrich the peptides containing lysine malonylation (Kmal), tryptic peptides dissolved in NETN buffer (100 mM NaCl, 1 mM EDTA, 50 mM Tris-HCl, 0.5% NP-40, pH 8.0) were incubated with pre-washed antibody beads (PTM-901, PTM Biolabs) at 4 °C overnight with gentle shaking. PTM-901 is specially designed for detecting malonyllysine [39,43]. The beads were washed four times with NETN buffer and twice with ddH_2O. The bound peptides were eluted from the beads with 0.1% trifluoroacetic acid. The eluted fractions were combined and vacuum-dried. The resulting peptides were cleaned with C18 ZipTips (Merck Millipore, Germany) according to the manufacturer's instructions, followed by LC-MS/MS analysis.

7. LC-MS/MS analysis

Three parallel analyses for each fraction were performed. Peptides were dissolved in 0.1% formic acid, directly loaded onto a reversed-phase pre-column (Acclaim PepMap 100, Thermo Fisher Scientific, USA). Peptide separation was performed using a reversed-phase analytical column (Acclaim PepMap RSLC; Thermo Fisher Scientific, USA). The gradient was comprised of an increase from 6% to 22% solvent B (0.1% formic acid in 98% acetonitrile) for 24 min, 22% to 35% for 8 min and climbing to 80% in 5 min then holding at 80% for the last 3 min, all at a constant flow rate of 300 nl/min on an EASY-nLC 1000 UPLC system (Thermo Fisher Scientific), the resulting peptides were analyzed by Q Exactive™ Plus hybrid quadrupole-Orbitrap mass spectrometer (Thermo Fisher Scientific, USA).

The peptides were subjected to NSI source followed by tandem mass spectrometry (MS/MS) in Q Exactive™ Plus (Thermo) coupled online to the UPLC (EASY-nLC 1000, Thermo Fisher Scientific, USA). Intact peptides were detected in the Orbitrap at a resolution of 70,000. The mass window for precursor ion selection was setting as 2 m/z. The charge state 2–5 was selected for MS/MS screening. Peptides were selected for MS/MS using NCE (normalized collision energy) setting as 30; ion fragments were detected in the Orbitrap at a resolution of 17,500. A data-dependent procedure that alternated between one MS scan followed by 20 MS/MS scans was applied for the top 20 precursor ions above a threshold ion count of 1.0E4 in the MS survey scan with 15.0 s dynamic exclusion. The electrospray voltage applied was 2.0 kV. Automatic gain control (AGC) was used to prevent overfilling of the Orbitrap; 5E4 ions were accumulated for generation of MS/MS spectra. For MS scans, the m/z scan range was 350 to 1800.

8. Database search

The resulting MS/MS data was processed using MaxQuant [50] with integrated Andromeda search engine (v.1.4.2). Tandem mass spectra were searched against 3728 *Bacillus amyloliquefaciens* coding sequences (NCBI Reference Sequence Database, Date: 2015.7.30, Version: NC_009725.1) concatenated with reverse decoy database. Trypsin/P was specified as cleavage enzyme allowing up to 4 missed cleavages, 5 modifications per peptide and 5 charges. Mass error was set to 10 ppm for precursor ions and 0.02 Da for fragment ions. Carbamidomethylation on Cys was specified as fixed modification and oxidation on Met, malonylation on Lys and acetylation on protein N-terminal were specified as variable modifications. False discovery rate (FDR) thresholds for peptide modification site, peptide and protein were controlled at 1%. Minimum peptide length was set at 7. The other parameters in MaxQuant were set to default values (Digestion mode: trypsin/P; Max missed cleavages: 4; First search PPM: 20; Main search PPM: 5; Max number of modifications per peptide: 5; Max charge: 5; Min peptide length: 7; Min razor & unique peptide: 1; Min score for modified peptides: 40; Peptides for quantification: Unique & razor peptides). The site localization probability was set as >0.75. We used WoLF PSORT [51], a subcellular localization predication software, to predict subcellular localization.

9. Analysis of enriched sequence pattern with malonylation

The software motif-x [52,53] was used to analyze the model of sequences constituted with amino acids in specific positions of modifier-21-mers in all identified malonylated protein sequences. Peptide sequences which were cut out 10 amino acids upstream of and downstream of an identified malonylation site from the identified protein sequences were used as foreground sequence for motif analysis. And all the database protein sequences were used as background. The other analysis parameters were set as follows: Modified acid amino "central character" was set as 'K' (lysine); foreground peptides sequence length "width" was set at 21; minimal number of peptide occurring in one motif "occurrences" was set at 20; motif analysis statistics test significance threshold value was set at 0.0000001.

10. Functional enrichment analysis

For each protein, three biological annotation information including gene ontology, pathway, and functional domain was retrieved. Gene ontology was annotated by UniProt-GOA (http://www.ebi.ac.uk.GOA). InterProScan was further used for new gene ontology assignment if there is no available information in UniprotGOA. The pathway information was collected from KEGG pathway database. The functional domain of each protein was annotated by InterProScan. The one-tailed Fisher's exact test was used to test the enrichment of the identified protein annotation against all annotation subjects. The annotation with a p-value <0.05 is considered significant.

11. Analysis of the distribution of malonylation sites in secondary structures and surface accessibility

Secondary structure analysis was performed using NetSurfP [54]. Only predictions with a minimum probability of 0.5 for one of the different secondary structures (coil, α-helix, β-strand) were considered for analysis. The mean secondary structure probabilities of the modified lysine residues were compared with the mean secondary structure probabilities of a control dataset containing all the lysine residues of all the malonylated proteins identified in this study. The p-values were calculated with the Wilcoxon test.

12. Malonyllysine sites conservation analysis

To determine the degree of evolutionary conservation of malonylation, a BLASTP analysis was used to compare malonylated protein sequences of *Bacillus amyloliquefaciens* against the protein sequences of 59 species from UniProtKB (http://www.uniprot.org/). Using the reciprocal best LAST hit approach, we determined the orthologous proteins among these genomes. For each orthologous group, MUSCLE (v3.8.31) was used to perform multiple sequence alignment. The conservation of malonylated lysine for each species was calculated by counting the total number of conserved malonylated lysine and the total number of conserved non-malonylated lysine. Lysine was considered to be conserved if the aligned locus is a lysine residue in both *B. amyloliquefaciens* and other multiple species. All lysine residues of the proteins identified in this study were considered as control. p-values were calculated using Fisher's exact test.

13. Protein-protein interaction analysis

All identified malonylated protein name identifiers were searched against the STRING database (version 10.0) for protein-protein interactions. Only interactions between the proteins belonging to the searched data set were selected, thereby excluding external candidates. STRING defines a metric called "confidence score" to define interaction confidence; we fetched all interactions that had a confidence score ≥ 0.7 (high confidence). Interaction network from STRING was visualized with Cytoscape. The network was analyzed for densely connected regions with molecular complex detection (MCODE), a graph theoretic clustering algorithm. 11 MCODE clusters were found. In order to further explore biological process of these MCODE clusters, GO category enrichment analysis was performed with each MCODE cluster. Three significance ($p < 0.05$) GO category related MCODE clusters were found.

3. Results and discussion

1. General features of the malonylome in B. amyloliquefaciens FZB42

Since there is no reference about the occurrence and the extent of protein malonylation in Bacillus, we firstly performed a pilot experiment: a Western blot analysis with B. amyloliquefaciens FZB42 proteins using anti-malonyllysine antibodies was conducted. The proteins prepared from six samples were compared with the difference in media (minimal medium: M9 medium and rich medium: LB medium), growth stages (exponential phase, transition phase, and stationary phase), or cell status (vegetative growth and biofilm). As a result, multiple protein bands spanning a wide mass range across the samples revealed the presence of diverse malonylated proteins. The highest degree of malonylation, indicated by abundant bands, was registered after 8 h growth in the liquid SE medium supplemented with soil extract (Supplementary Fig. S1). This medium has been used previously [49], in order to provide an environment more close to natural soil. However, the degree of malonylation seemed to be more related to growth stage rather than to medium ingredients, because at the vegetative growth stage (OD600 = 1.0) a similar band abundance happened in both LB medium and SE medium, whereas in the same SE medium there were obviously higher malonylation degree at the 8th hour than at the earlier and the later time points (Supplementary Fig. S1). We thus selected the sample from the 8th hour for next malonylome profiling, although the relative high malonylation degree at this time point may need to be confirmed further.

The peptides enriched with malonyllysine antibodies were profiled with 2D-LC-MS/MS and the obtained spectra were used to search the *B. amyloliquefaciens* databases [2]. For quality control, the mass error of all identified peptides and their peptide length distribution were checked. The distribution of mass error was near zero and most of them were <5 ppm, suggesting a good accuracy of our MS data (Supplementary Fig. S2a). The length of most peptides was distributed between 7 and 30 amino acids and agreed with the property of tryptic peptides (Supplementary Fig. S2b). A total of 382 proteins were found to be malonylated on 809 unique lysine sites (see Table 1 in [55]), corresponding to ~2.1 sites per protein. Possibly due to our specific extraction method, the majority of malonylated proteins (~90%) was cytoplasmic; the remaining were either extracellular or membrane proteins (Supplementary Fig. S2c). Using the spectra of the peptides enriched, we also searched the database for other PTM types structurally similar to lysine malonylation, like acetylation, succinylation, and propionylation. Compared with 887 (4.82%) of the peptides identified to contain malonylation, 9 (0.05%), 28 (0.16%), and 6 (0.03%) of peptide were found to have acetylation, succinylation, and propionylation, respectively (see Table 2 in [55]). This result indicates a good specificity and sensitivity of the malonyllysine antibodies.

The identified malonylated proteins accounted for ~10% (382/3698) of the proteome of *B. amyloliquefaciens* FZB42. This number is less than that of the acetylated proteins recently identified in *B. amyloliquefaciens* subsp. *amyloliquefaciens* DSM7 [28], but was more than the number of succinylated proteins detected in *B. subtilis* [17,19,32]. Among the 382 malonylated proteins, 54% contained a single lysine malonylation (Kmal) site; 22% contained two Kmal sites; and 9% contained three sites (Supplementary Fig. S2d). The polyketide synthases, BaeR, BaeN, BmyA, and BaeM possessed >10 Kmal sites. Bacillaene synthetase R (BaeR) was the most heavily malonylated protein carrying 17 Kmal sites.

To identify specific sequence patterns present in the target sequences of malonylation, we compared the position-specific amino acid frequencies of sequences surrounding the malonylated lysine with those of all lysine residues occurring in the *B. amyloliquefaciens* FZB42 proteome. We thus defined six significantly enriched Kmal site sequences for 327 unique sites, accounting for 40% of Kmal sites identified (Supplementary Fig. S3). For five of these significant patterns, positively charged arginine or lysine residues were enriched in close vicinity to the malonyllysine sites, resembling the accumulation of positively charged amino acids in the acetylation sites of *S. roseosporus* [14]. The over-presented patterns identified here imply that amino acid residues with positive charge may be functionally important for malonylation.

2. Lysine malonylation involved a wide range of functions in B. amyloliquefaciens

Using a classification system adapted from *B. subtilis* [56], we classified the 382 malonylated proteins into several functional groups (Fig. 1a). Except that nearly 10% of proteins were with unknown function, lysine malonylation was detected on proteins involved in a wide spectrum of biological functions. The details of functional categories of proteins are summarized in Table 3 in [55].

Accounting for ~38% of the detected malonylome, 145 proteins are involved in intermediary metabolism. Among them, the largest portion of the proteins were the enzymes involved in central carbon metabolisms such as Embden–Meyerhof–Parnas (EMP) pathway, pentose phosphate pathway (PPP) and the tricarboxylic acid cycle (TCA) (see Table 3 in [55]). Nearly all of the enzymes involved in the EMP pathway were malonylated including those critical for limiting reaction rate: 6-phosphofructokinase (PfkA), phosphoglycerate kinase (Pgk) and pyruvate kinase (Pyk). Twenty proteins related to the metabolism of lipids were also malonylated containing a total of 45 Kmal sites (see Table 3 in [55]). These proteins were involved in either fatty acid elongation or fatty acid β-oxidation. The two proteins involved in fatty acid β-oxidation, FadN and FadE, possess 10 and 8 Kmal sites, respectively. Since the above carbonhydrates are mainly related to energy biosynthesis, together with the fact that another set of 16 proteins (see Table 3 in [55]) associated with electron transport chain and ATP synthesis were also malonylated, this leads us to infer that malonylation may be important in governing energy generation of bacteria.

The proteins involved in information pathway represented the second largest group comprising around 22% (85 proteins) of all the malonylated proteins. The members of this group are devoted to the genetic information flowing process from DNA to proteins. Nearly 60% of the proteins (49 proteins) were related to protein synthesis: they are 14 aminoacyl-tRNA synthetases, four elongation factors (FusA, TufA, Tsf, and Efp), three initiation proteins (Fmt, InfB, and InfC), one ribosome recycling factor (Frr), as well as 27 ribosomal proteins. Notably, on the elongation factor FusA there were 10 Kmal sites. In addition, four proteins (GroEL, GroES, DnaK, and Tig) involved in protein folding and three involved in protein modification were also malonylated. This result suggests a potential role of lysine malonylation in controlling protein synthesis. The second largest subgroup of the information pathway proteins are those involved in RNA synthesis. Nineteen proteins are the members of this subgroup, including RNA polymerase (RpoA, RpoB, RpoC, RpoD, and RpoE) and a series of transcriptional regulators such as AbrB, Spo0A, and CodY.

To explore the possible functional roles shared by the malonylated sites, we performed enrichment analysis based on the Gene Ontology (GO) database. While instead of analyzing the whole malonylated proteins, we examined the distribution of malonylated peptides in various protein domains in order to gain a finer insight into their functional enrichment. It reveals that Kmal sites were significantly enriched in the domains such as the phosphopantetheine-binding domain and the beta-ketoacyl synthase domain of polyketide synthase, thiolase-like domain, nucleic acid-binding OB fold, aldolase-type TIM barrel, and acyl carrier protein-like domain (Fig. 1b). This result agree with the distribution of the malonylated proteins in various proteins, but pinpoints more precisely the preferred location of malonyl groups on the proteins and implies possible specialized functions of malonylation.

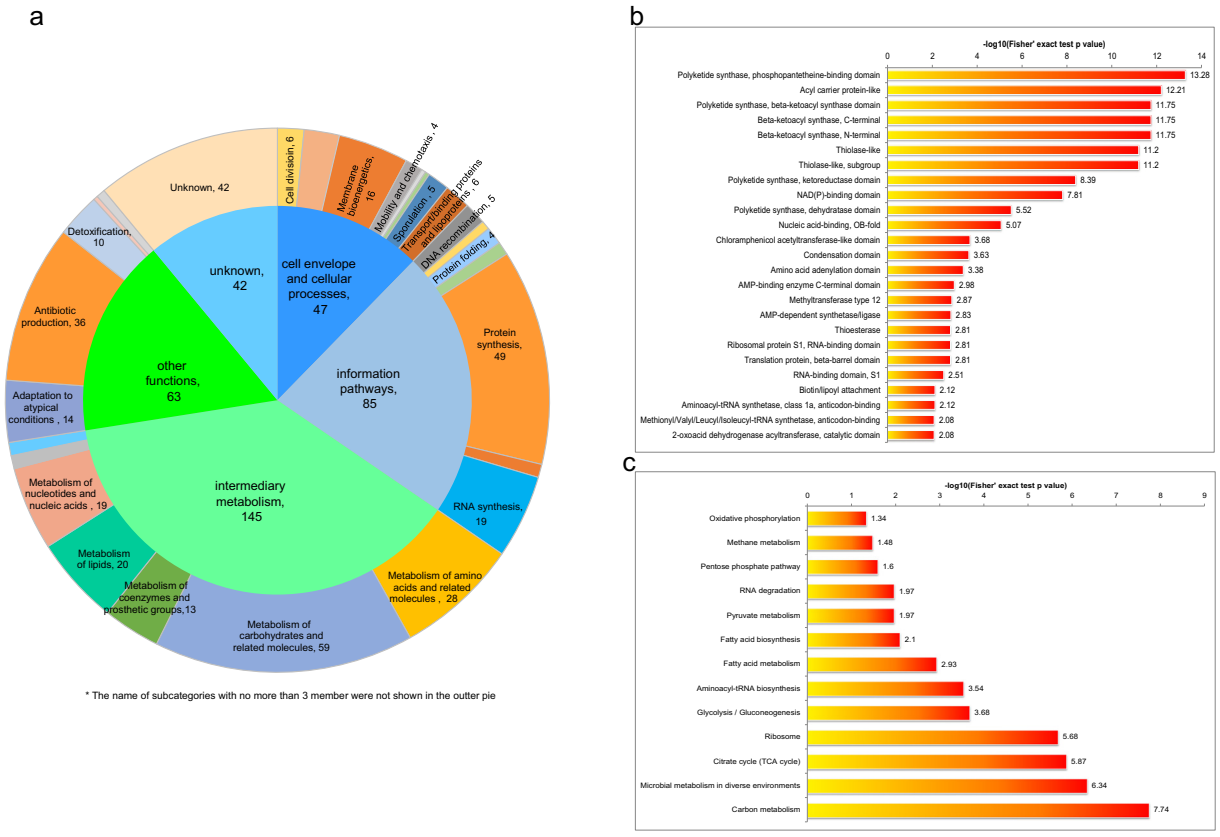

Fig. 1. Functional category analysis of the malonylated proteins/domains in B. amyloliquefaciens FZB42. (a) Distribution of malonylated proteins in various functional categories. The malonylated proteins were classified into various functional categories according to reference [56]. While the inner pie displayed the main functional categories, the outer pie indicated subclasses of the main functional categories. The classification of each malonylated protein identified in B. amyloliquefaciens FZB42 was shown in Table 3 in [55]. (b) Statistically enriched domains of the malonylated proteins. The ratio of Kmal sites locating in the domain to all Kmal sites was compared with the ratio of proteins containing the malonylated domains to all proteins in the database. The one-tailed Fisher's exact test was used to test the enrichment and the result with p-value <0.05 is considered significant. (c) KEGG (Kyoto Encyclopedia of Genes and Genomes) pathways that were statistically overrepresented were identified using Fisher's exact test method. The length of each bar represents the statistical significance, plotted as the -log10(p-value).

In addition, KEGG enrichment analysis was performed in order to gain an insight into the connections among the malonylated proteins. We observed that 13 KEGG pathways were highly enriched (Fig. 1c and Supplementary Fig. S4), including glycolysis/gluconeogenesis, TCA cycle, pentose phosphate pathway, fatty acid metabolism and biosynthesis, oxidative phosphorylation, RNA degradation and methane metabolism. In general, the pathway enrichment result indicates a possible role of lysine malonylation in many reactions especially in carbon metabolism.

Some of the enriched functional categories/pathways of the malonylated proteins have also been observed in eukaryotes. For example, the mammalian malonylomes exhibit a close relationship between lysine malonylation and glycolysis/gluconeogenesis, where malonylation suppresses the enzymatic activity of GAPDH (glyceraldehyde-3-phosphate dehydrogenase) [36]. In addition, the enriched pathways were also shared by the proteins with other PTM types: the proteins involved in protein synthesis are abundantly acetylated in *S. roseosporus* [14]; acetylation is well known to target many enzymes of central carbon metabolism in not only eukaryotes but also various prokaryote species such as *E. coli*, *Salmonella*, and *Thermus thermophilus*, *B. subtilis*, *B. amylolyquefaciens*, and *S. roseosporus* [14,17,19,23,25,32,57,58]. The occurrence of succinylation in the cycle and fatty acid metabolisms has also been reported [32,35]. However, lysine malonylation seemed absent in those RNases (RNase R, RNase E, and RNase J), which are targets of acetylation [14,59]. In general, the different PTMs displayed some overlapping functional targets.

3. Polyketide synthases (PKS) and non-ribosomal peptide synthetases (NRPS) were highly malonylated

Polyketides and nonribosomal peptides are two families of natural products biosynthesized in a similar manner by multi-modular enzymes acting in assembly line arrays. The monomeric building blocks are organic acids or amino acids, respectively [60]. *B. amyloliquefaciens* FZB42 is an efficient producer of polyketides and cyclic lipopeptides, including some (difficidin, macrolactin, and bacillomycin D) which do not occur in non-plant-associated *B. amyloliquefaciens* and *B. subtilis* strains [2,3]. Besides three malonylated proteins involved a ribosomally synthesized peptide plantazolicin, a total of 33 enzymes, accounting for nearly 8.6% of the 382 malonylated proteins, were involved in the nonribosomal synthesis of seven antibiotics: bacillaene, difficidin, macrolactin, bacillomycin D, fengycin, surfactin, and an unknown peptide. The 33 enzymes contained 128 Kmal sites, corresponding to a mean of 3.8 sites per protein, which is significantly higher than the average level of 2.1 Kmal sites per protein.

The bacillaene synthase in FZB42, encoded by a >70 kb gene cluster [47], is a mega complex composed of 15 enzymes, some of which possess multiple functional domains. The complex is characterized by the presence of discrete acyltransferases acting in trans (BaeC, D, E), hybrid NRPS/PKS enzymes BaeJ and BaeN [46,47], and polyketide synthases BaeL, BaeM and BaeR [3,61]. BaeR, BaeN, and BaeM were the most malonylated proteins detected in this study,

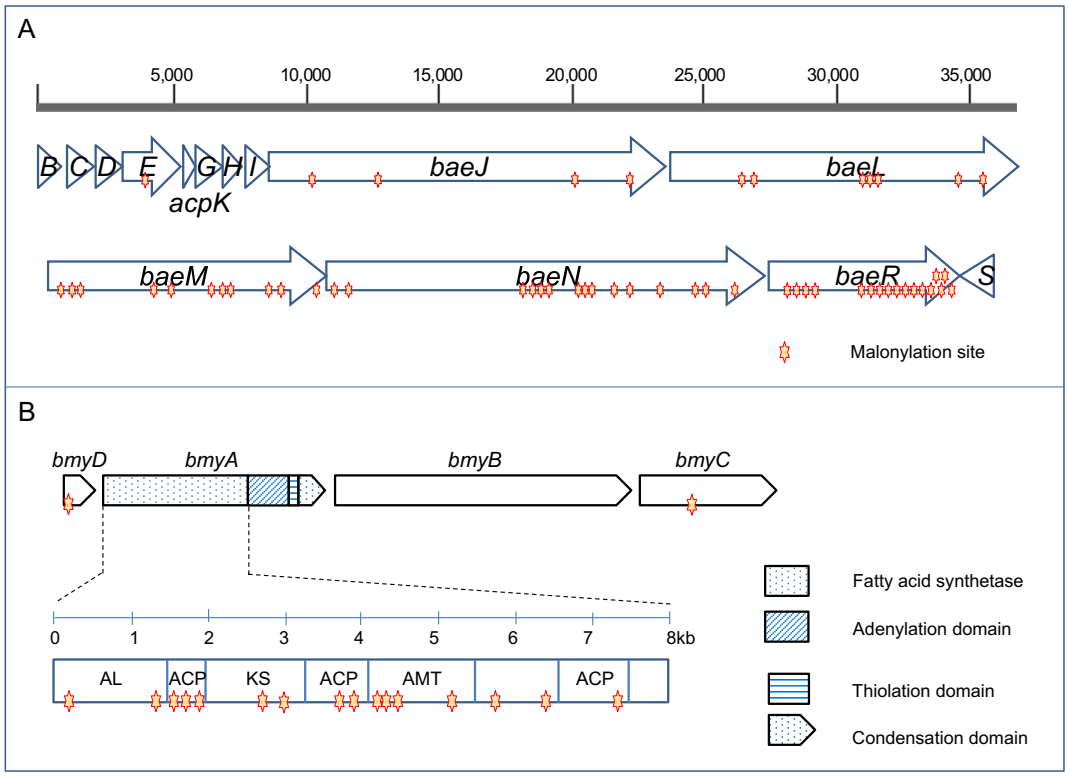

Fig. 2. Schematic presentation of Kmal sites in the mega enzyme complexes of the synthetase for bacillaene and bacillomycin D. The gene clusters for the enzyme complexes involved in the nonribosomal synthesis of bacillaene (a) and bacillomycin D (b) are depicted as the arrows in tandem. The malonylated sites are indicated as stars in the genes; their locations are approximately proportional to the linear distance relative to each other on the enzymes. The predicted functional domains of BmyA are also noted. AL: acyl coenzyme A ligase domain; ACP: acyl carrier protein domain; KS: β-ketoacyl synthetase domain; AMT: aminotransferase domain.

containing 17, 15 and 11 Kmal sites, respectively (Fig. 2a, and see Table 1 in [55]). Compared with other domains of the enzymes, such as KR (ketoreductase) domain and TE (thioesterase) domain, around one third of the Kmal sites on BaeR, BaeM, and BaeN were located on the ACP and KS domains. This possibly suggests a preference of malonylation on ACP domains and KS domains.

This preference seems also true to BmyA, the second highest malonylated protein with 16 Kmal sites. BmyA is a member of the gene cluster responsible for bacillomycin D synthesis. The gene cluster consists of four open reading frame (ORF): the first ORF encodes a putative malonyl coenzyme A transacylase, BmyD, which participates in fatty acid synthesis; the other ORFs encode the hybrid PKS/NRPS enzyme, BmyA, and the NRPS enzymes BmyB and BmyC [44,62]. While BmyD and BmyC each contained one Kmal site and BmyB contained no Kmal site, all the 16 Kmal sites of BmyA (3982 AA) were concentrated within the part homologous to fatty acid synthetase (Fig. 2b, and see Table 1 in [55]). Three acyl carrier proteins (ACP) domains possessed six Kmal site, and the β-ketoacyl synthetase (KS) domain possessed two Kmal sites. Besides, there were two Kmal sites on the AL domain, highly similar to long chain fatty acid-CoA ligase, and another four sites on the AMT domain, homologous to glutamate-1-semialdehyde aminotransferase.

The ACP domains are known to be associated with binding of phosphopantetheine, which is pivotal for the PKSs serving as a "flexible arm" to deliver a substrate from one active site of the enzyme complex to the next one [63]. The KS domains have an SH group on a cysteine side-chain and catalyze Claisen condensation by handing over the nascent polyketide chain from the ACP domain of the previous module to the KS domain of the current module [63]. This is an irreversible key step, forming carbon to carbon bond, in fatty acid and polyketide synthesis [64]. The malonylation on ACP domains indicates their possible important role in regulating reaction rate of polyketide synthesis.

Malonyl-CoA was previously assumed as the donor of malonyl group for lysine malonylation, which has led to the first identification of malonylome in eukaryotes and the further investigations [34,65]. Malonyl-CoA is known to play a key role in chain elongation in fatty acid and polyketide biosynthesis in bacteria. In FZB42, for example, the macrolactin skeleton is synthesized by extension of an acetyl starter unit by successive Claisen condensations with Malonyl-CoA [45]. This knowledge implied a possibility that the diverse PKSs/NRPSs in FZB42 could be malonylated. Such reasoning initiated this study and was confirmed by the results reported here. Although the roles of these Kmal sites still remain elusive, their relative high occurrence in the enzymes suggests the potential importance of malonylation in the non-ribosomal synthesis of polyketides and hybrid lipopeptides. In future, a deeper understanding of the mechanism of malonylation regulation, for example, identification of the enzymes responsible for lysine malonylation and demalonylation in bacteria, may help to utilize the bacteria as an efficient factory for antibiotic production [34–36].

4. Lysine malonylation of proteins related to microbe-plant interactions

The molecular mechanism of interaction with host plants has been a research focus of rhizobacteria for a long time. As a representative of PGPR strains, the FZB42 genes implicated in the interaction with plants have been carefully explored in our previous studies [2,41,48,66,67]. Here we found that some proteins involved in these interactions were malonylated. A vital group of these proteins included those involved in antibiosis, which has been discussed above. Antagonistic activity against phytopathogens of the antibiotics such as polyketides and

nonribosomally synthesized lipopeptides is a major mechanism of biocontrol activities of beneficial rhizobacteria. In addition, forming biofilms on plant roots is another barrier against attacks of phytopathogens. We found that YmcA, an important master regulator of biofilm formation [68,69], and LuxS, required in biofilm formation [70,71], were also malonylated.

Notably, a set of proteins, which previously found induced by maize root exudates [48], were malonylated (see Table 4 in [55]). This set of induced genes includes, besides the genes involved in antibiotic synthesis and central carbon metabolism, some other genes. For example, the *iol A-J* gene products are responsible for utilizing of inositol, which is abundant in soil in the form of hexaphosphate (phytate). Inositol can be degraded by soil bacteria as nutrient source. Six proteins (IolA, IolB, IolC, IolG, IolH, IolI) encoded by the *iol* operon as well as the regulator IolS were malonylated at 14 lysine sites. Furthermore, 1) the enzyme GlvA, whose gene is the highest induced by root exudates and responsible for maltose utilization; 2) the enzyme LuxS, implicated in quorum sensing [70,71], an important signaling process related to biofilm formation; 3) the enzymes BdhA (YdjL), AcoA, and AcoC, involved in synthesis of acetoin and 2.3 butanediol, the volatiles known to stimulate plant growth and systemic resistance of plants [72–75]; and 4) the detoxifying enzymes removing free oxygen radicals in cells, like superoxide dismutase (SodA) and thioredoxin (TrxA), which are crucial for rhizobacterial adaptation in rhizosphere [1,2], were also malonylated. A set of the malonylated proteins involved in plant-microbe interactions were summarized in Fig. 3.

The above malonylated proteins are important for rhizobacterial adaption to plant environment or for their beneficial activities to plants. Thus, we presumed that lysine malonylation may also be important to microbe-plant interactions. To provide evidence for this, the locations of malonyllysines in some of the proteins were further analyzed. The possible effect of malonylation on their structures or activities was found for several proteins. For example, malonylated K97 of *myo*-inositol dehydrogenase IolG is corresponding to the same site of inositol dehydrogenase from *B. subtilis* (BsIDH) (Fig. 4a). K97 is part of the highly conserved C95EKP motif and one member of the important catalytic triad (Lys97, Asp172, and His176) involved in the catalytic activity of BsIDH [76]. K97 may be responsible for proper orientation of the nicotinamide ring and the substrates or involved in a proton relay [76]. Another example is LuxS carrying the malonylated K124 and K130, which are comparable to K124 and K130, respectively, in *B. subtilis* (Fig. 4b). K124 and K130 of *B. subtilis* are in the active site of LuxS with the presence of a Zn^{2+} atom. The chain from 118 to 132, including the important residue Cys126, underpins the Zinc-binding site of LuxS [77]. The malonylation of K124 and K130, near to Cys-126, may affect the coordination of the metal. Further, as the third example, the malonylated K54 of TrxA was also found near the active site (segments 24–34 and 57–73), according to the protein structure of *B. subtilis* (Fig. 4c) [78].

We also analyzed the protein TufA, which was induced by root exudates and bears three Kmal sites (K239, K266, and K316), for the significance of malonylation. The elongation factor TufA is known to recognize and transport non-initiator aminoacyl-tRNA to the A site of ribosomes in the elongation cycle. The Lys237 (corresponding to K239 in FZB42) in *E. coli* was shown to be cross-linked to a 3′-oxidized tRNA in a complex with GTP [79]. The Lys263 of *E. coli* (K266 in FZB42) has a very reduced reactivity but its environment is highly altered upon the conformational change in EF-Tu, which takes place during nucleotide exchange [80–82]. Further, Lys263 and its neighboring Phe261, Arg262 surround the binding sites of several antibiotics artificially designed to act against *Clostridium difficile* infection (Fig. 4d) [83–85]. This information further supported the potential biological significance of malonylation identified.

5. Functional relationships between proteins with malonylation and other PTMs

Using the PTM information from the model organism *B. subtilis*, we found that 71.2% of the malonylated proteins were also post-

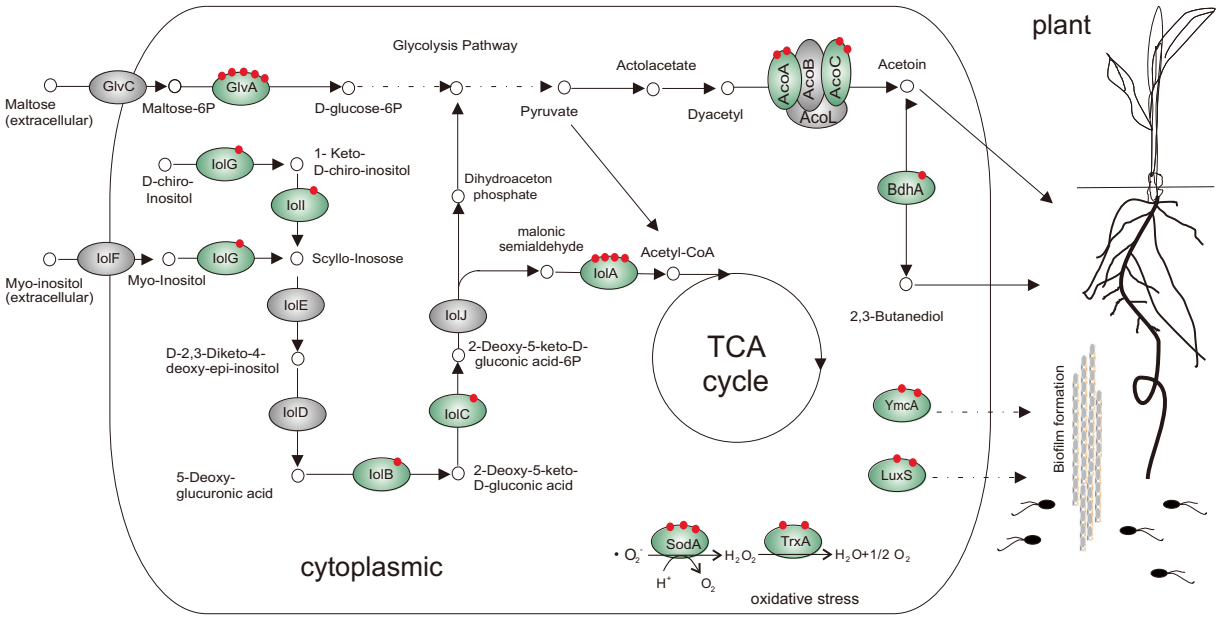

Fig. 3. Malonylated proteins reported being involved in plant-microbe interaction. The malonylated proteins are shown in green ovals with one red circle representing one malonyllysine site. The proteins shown are 6-phospho-alpha-glucosidase (GlvA), acetoin dehydrogenase E1 component (AcoA), and acetoin dehydrogenase E2 component (AcoC), acetoine/butanediol dehydrogenase BdhA (YdjL), D-chiro-inositol transport protein (IolF), 2-keto-myo-inositol dehydratase (IolE), 3D-(3,5/4)-trihydroxycyclohexane-1,2-dione hydrolase (IolD), 5-deoxy-D-glucuronate isomerase (IolB), 2-deoxy-5-keto-D-gluconic acid kinase (IolC), methylmalonate-semialdehyde dehydrogenase (IolA), master regulator of biofilm formation (YmcA), autoinducer-2 production protein (LuxS), superoxide dismutase (SodA), and thioredoxin (TrxA).

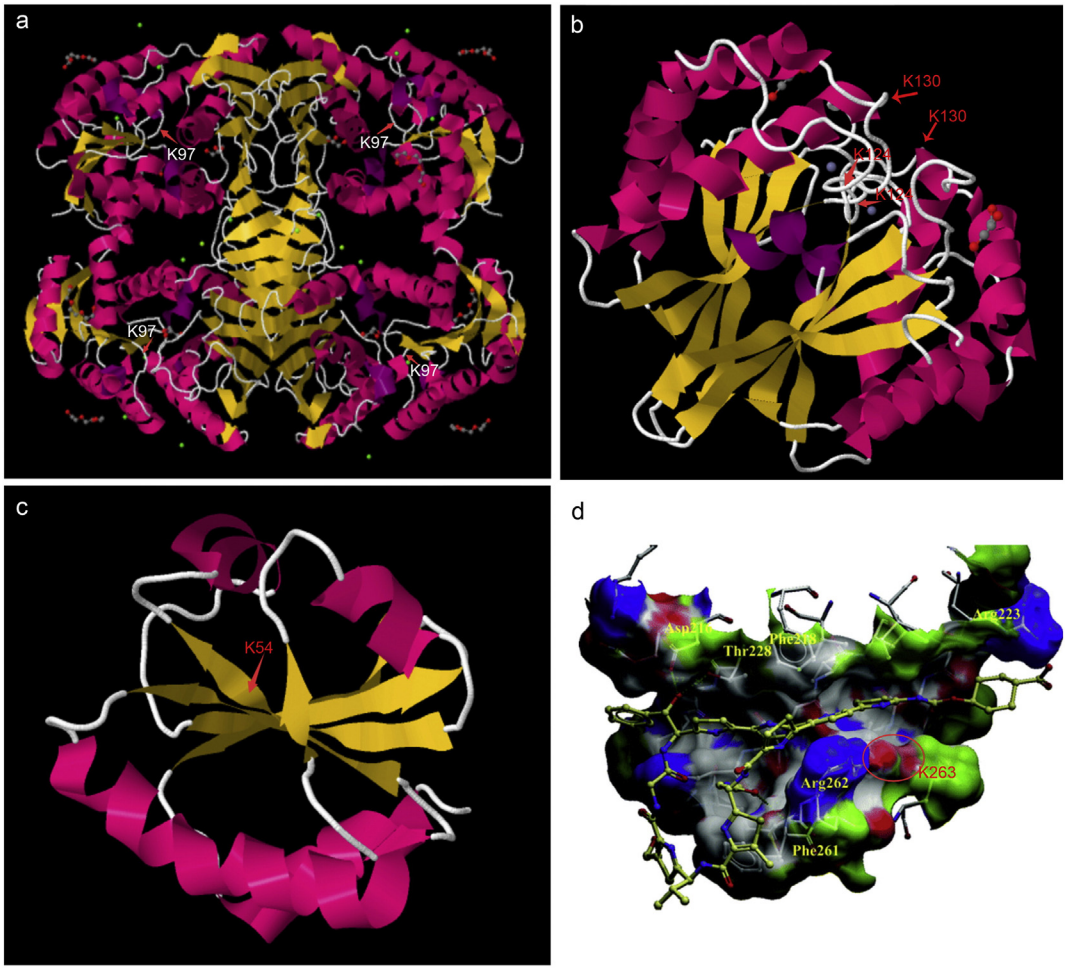

Fig. 4. Structures of a set of proteins with identified malonyllysine(s). Three-dimensional structures of the proteins with a malonylated lysine residue(s) indicated by red arrows or a red circle were shown. (a) Homo-4-mer *B. subtilis myo*-inositol dehydrogenase IolG bears the malonylated K97 locating at a catalyzing site; (b) Homo-2-mer *B. subtilis* s-ribosylhomocysteine lyase LuxS bears malonylated K124 and K130 locating at an active site with the presence of a Zn^{2+} atom (the gray circle); (c) *B. subtilis* thioredoxin TrxA bears the malonylated K54; (d) *E. coli* elongation factor TufA bears malonylated K237 (corresponding to K239 in FZB42) and K263 (corresponding to K266 in FZB42). Lys263 indicated by the red circle and it neighboring Phe261, Arg262 surround the binding sites of a ligand LFF571 selected against *Clostridium difficile* infection [82]. The first three structures were taken from PDB database, while the TufA structure with its ligand was taken from reference 82.

translationally modified by other chemical groups (acetylation, succinylation or phosphorylation) (see Table 5 in [55]). This raises a possibility of functional cross-talks between the different types of PTMs. To comprehend the relation profile between the modified proteins, a protein-protein interaction network was established for the differently modified proteins (Fig. 5). In the network the connections between these proteins form some clusters, suggesting closer interactions within each of them. The clusters included several functional categories of proteins significantly enriched as follows: fatty acid biosynthesis, central carbon metabolism, polyketide synthases (beta-ketoacyl synthetase domain) and ribosome related proteins. These clusters illustrate the functional relatedness of the modified proteins.

The proteins carrying three overlapping modifications (malonylation, acetylation, and succinylation) were mainly distributed into the functional categories of translation machinery and central carbon metabolism. The surfactin synthetase SrfAB is the most heavily modified protein containing a total of 35 modification sites of all the four PTM types. The complicated interaction network among the proteins and some of them with strong modifications by different PTMs suggest a complex effect of their modifications and possibly concerted actions in some cellular processes.

6. Malonylation occurs with higher surface accessibility

In order to find a possible relationship between the Kmal sites and protein secondary structures, we performed a structural analysis of all identified malonylated proteins. The mean probability of Kmal sites located at a certain type of secondary structures (α-helixes, β-strands, or coils) was compared with that of all lysine sites located at the structure. The result suggests that Kmal sites does not prefer certain secondary structures (Fig. 6a), consistent with what was observed for protein acetylation [17,86], although some argue that lysine acetylation preferred coil rather than α-helixes and β-strands [14,25,28]

The structural analysis also allows us to assess surface accessibility of these malonylation sites. It is shown that the average surface accessibility of the malonyllysines was significantly higher ($p < 0.001$) than that of all lysines (Fig. 6b). This indicates that the Kmal sites are preferably located on the surface of proteins and probably occur after maturation of the proteins. We suspect that the preferred distribution of Kmal sites on protein surfaces may be an advantage to the biosynthesis of fatty acids and polyketides. In the process of production of these molecules, the association of elongating fatty acid chains or polyketide chains with their synthases may increase the hydrophobicity of the mega complex, thus interfering

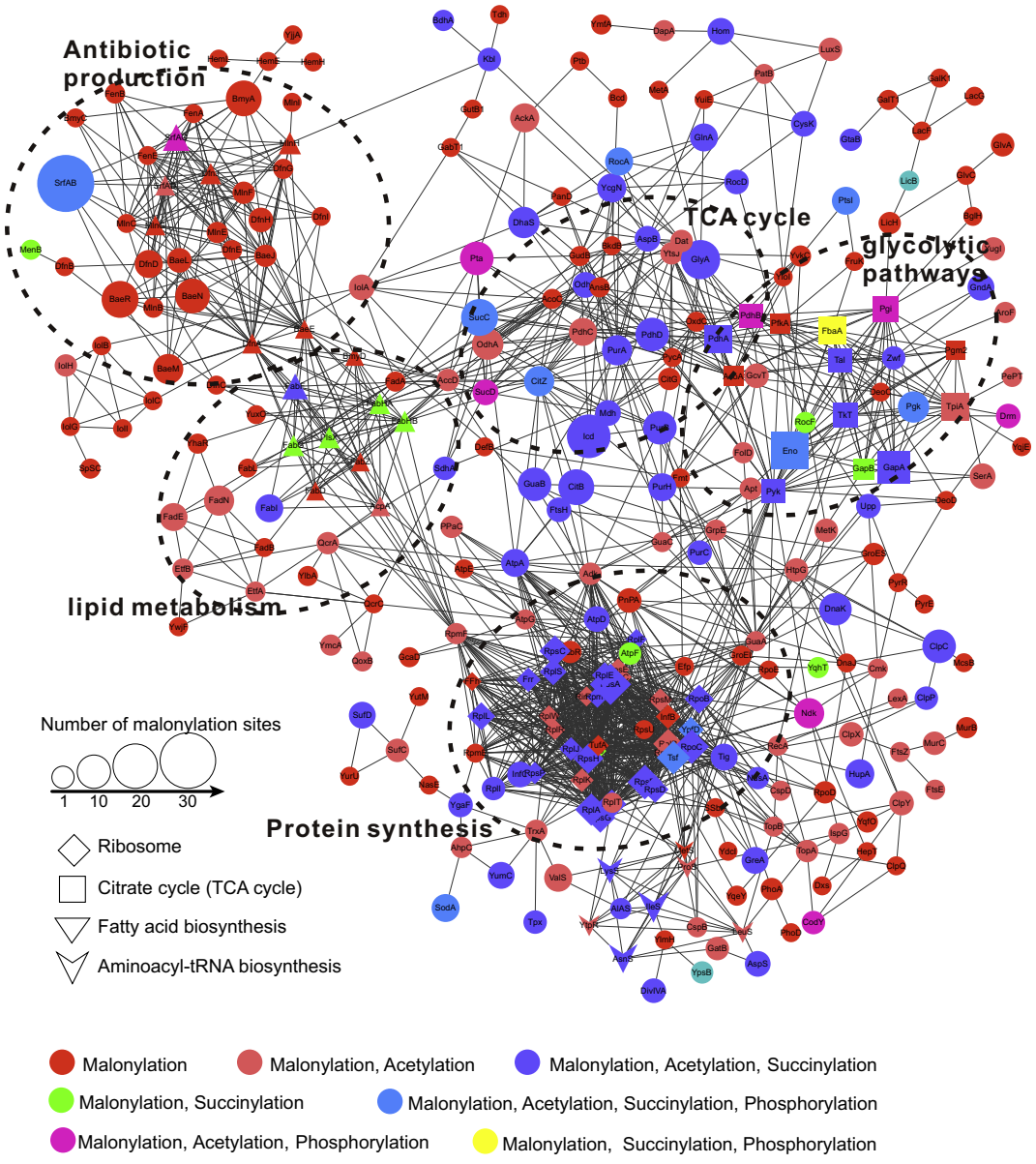

Fig. 5. Interaction network of the proteins with different PTM types. The interactions among the malonylated proteins with other previously reported PTM types were established. Each protein is indicated by a circle, the size of which is proportional to the number of modification sites on the protein. Any recorded relation between two proteins is indicated by a connecting line. Proteins in the significantly enriched ($p < 0.05$) functional group according to GO category are differently underlined. The proteins with different types of modification are indicated by different colors.

with their normal assembly in an aqueous environment. A possible mechanism of balancing this hydrophobicity is to enhance protein surface accessibility, for example, with the presence of lysine malonylation.

7. Malonyllysine sites are conserved in many bacteria but not in archaea

The degree of malonylation conservation could be a good indicator of the extent of how malonylation affects proteins. To define this, we examined the evolutionary conservation of malonylated and non-malonylated lysines in diverse species. In total, we selected 59 species covering five important groups in the three domains of life. These species include the representatives of Bacilli, which are the low GC% Gram-positive bacteria and the relatives of FZB42; the representatives of actinobacteria, which are one of the dominant bacterial phyla and also Gram-positive but with high GC%; the representatives of proteobacteria, which is a major group of Gram-negative bacteria; the representatives of different archaea, and several eukaryotes which are most commonly used as model organisms such as *Caenorhabditis elegans*, *Drosophila melanogaster*, *Mus musculus*, *Homo sapiens*, and *Arabidopsis thaliana* (Fig. 7). For each group, the species representing the major subgroups were selected.

The result revealed that in some species of the Bacillus group, the Actinobacteria group and the proteobacteria group the malonylated lysines were significantly more conserved than the non-malonylated lysines (Fig. 7). This is also the case in some eukaryotes, e.g. *Homo sapiens* and *Drosophila*. Using the existing malonylomes [36–39,43], we could sum up 89 conserved Kmal sites that are present in other bacteria (*E. coli* and *Saccharopolyspora erythraea*), human, or mouse (see Table 6 in [55]). The higher degree of conservation in malonylated lysines indicates a stronger selective pressure to

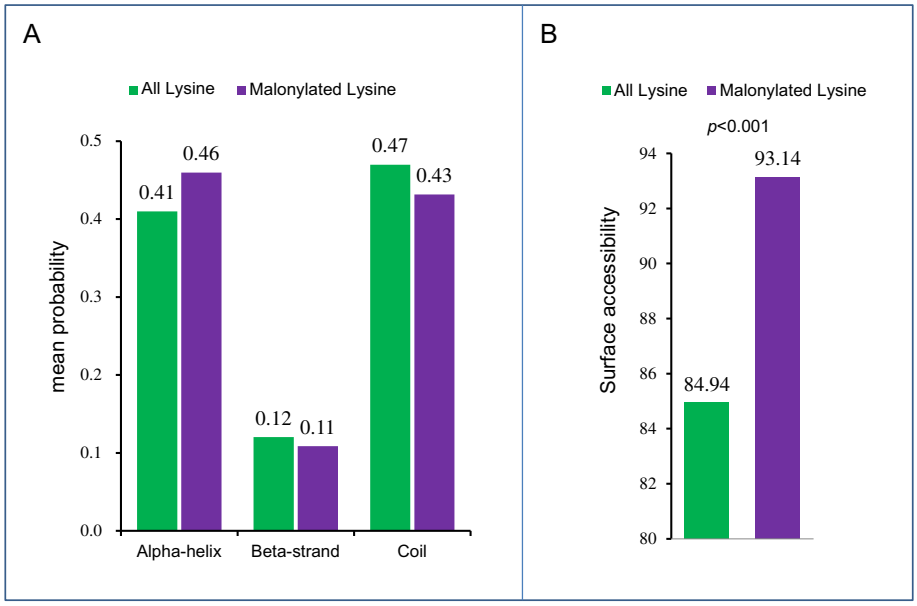

Fig. 6. Distribution of Kmal sites in different secondary structures (a) and their effect on surface accessibility (b). (A) Distribution of the malonylated lysines and all lysines of *B. amyloliquefaciens* FZB42 in different protein secondary structures were compared. (B) Surface accessibility of the malonylated lysines and all lysines of *B. amyloliquefaciens* FZB42 were compared. The *p*-values were calculated with the Wilcoxon test.

maintain the malonylated lysines. This may be due to conserved functional roles of Kmal in cells, although we would not exclude the alternative possibility; e. g. the protein regions where Kmal sites occur may be more structurally conserved.

By contrast, in all chosen species of archaea there was no statistical difference in the conservation of malonylated and non-malonylated lysines (Fig. 7). The absence of conserved sites in archaea may reflect their phylogenetic distance and physiological difference from bacteria. For example, a number of malonylated proteins are involved in lipid metabolism; however, it is well known that archaeal lipids lack fatty acids. This difference may partially account for the reason why Kmal sites were conserved in bacteria but not in archaea species. However, the finding needs be interpreted with enough prudence due to still limited observation.

4. Conclusion

Our data showed that lysine malonylation occurs on a number of *B. amyloliquefaciens* subsp. *plantarum* FZB42 proteins and targets a wide range of biological functions. Those conserved functions like central carbon metabolism, fatty acid metabolism, and protein synthesis as well as those related to biocontrol activities and plant bacteria-interactions, a remarkable feature of this species, suggests the possibility that malonylation may play an important role in governing such processes. In general, our results provide a starting point for further elucidating the functions of malonylation in regulating the physiology of rhizobacteria, the model organism *B. subtilis*, and many other prokaryotes. On the other hand, since we restricted our detection of malonylation peptides to one condition, it is very

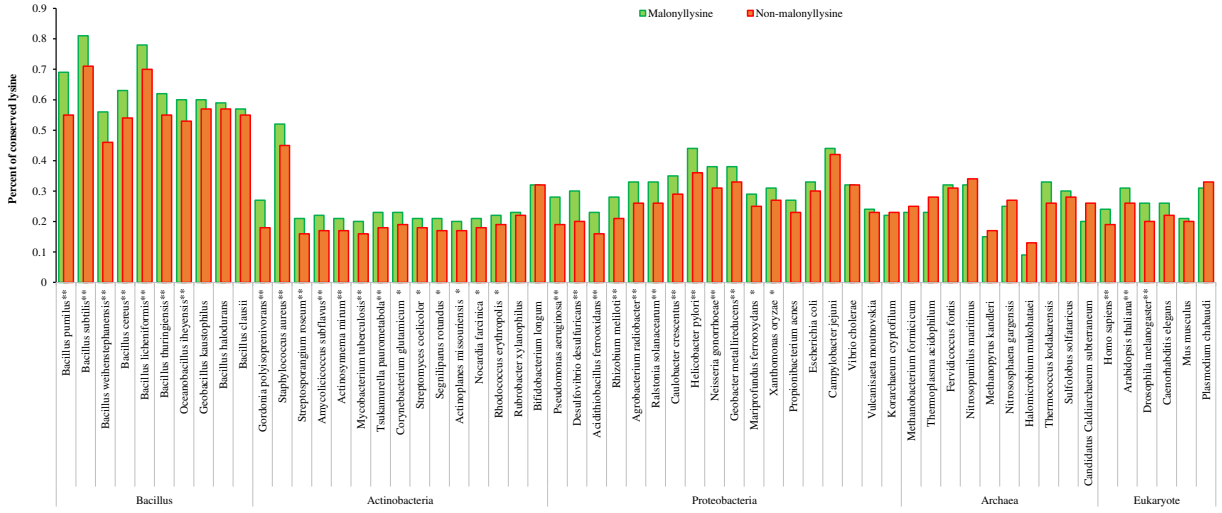

Fig. 7. Evolutionary conservation analysis of Kmal sites across various species. Evolutionary conservation was analyzed of the malonylated lysines and the non-malonylated lysines across various species in some major categories (*Bacillus*, Actinobacteria, Proteobacteria, Archaea, Eukaryotes) of the Three-domain System. *p*-values were calculated for each comparison using Fisher's exact test. The species with significant malonyllysine conservation were indicated by * ($p < 0.05$) or ** ($p < 0.01$).

likely that many malonylation sites remain unidentified. A systematic screening of the full map of malonylation sites is still necessary in future. Other important questions, e.g., what are the enzymes responsible for malonylation/demalonylation and the interactions between malonylation with other PTMs, also await further investigations. These explorations will contribute to gradually decipher the largely unknown part of the malonylation world.

Author contributions

B·F conceived the study, analyzed the data and wrote the manuscript draft; Y.L.L collected the samples and revised the manuscript; L.L, X.J.P, and C·B analyzed the bioinformatic data and revised the manuscript; X.Q.W and R.B financially supported the study and finalized the manuscript.

Conflict of interest

The authors declare that no conflict of interest exists.

Acknowledgement

The financial support by the National Natural Science Foundation of China (No. 31100081), Natural Science Foundation of Jiangsu Province (No. BK20151514), and the Priority Academic Program Development (PAPD) of Jiangsu Higher Education Institutions is gratefully acknowledged.

Appendix A. Supplementary data

Supplementary data to this article can be found online at http://dx.doi.org/10.1016/j.jprot.2016.11.022.

References

[1] B.J.J. Lugtenberg, F. Kamilova, Plant-growth-promoting rhizobacteria, Annu. Rev. Microbiol. 63 (2009) 541–556.
[2] X.H. Chen, A. Koumoutsi, R. Scholz, et al., Comparative analysis of the complete genome sequence of the plant growth-promoting bacterium *Bacillus amyloliquefaciens* FZB42, Nat. Biotechnol. 25 (9) (2007) 1007–1014.
[3] X.H. Chen, A. Koumoutsi, R. Scholz, et al., More than anticipated - production of antibiotics and other secondary metabolites by *Bacillus amyloliquefaciens* FZB42, J. Mol. Microbiol. Biotechnol. 16 (1–2) (2009) 14–24.
[4] L. Katz, Manipulation of modular polyketide synthases, Chem. Rev. 97 (7) (1997) 2557–2576.
[5] C. Dai, W. Gu, p53 post-translational modification: deregulated in tumorigenesis, Trends Mol. Med. 16 (11) (2010) 528–536.
[6] A.P. Lothrop, M.P. Torres, S.M. Fuchs, Deciphering post-translational modification codes, FEBS Lett. 587 (8) (2013) 1247–1257.
[7] J.A. Cain, N. Solis, S.J. Cordwell, Beyond gene expression: the impact of protein post-translational modifications in bacteria, J. Proteome 97 (2014) 265–286.
[8] S. Prabakaran, G. Lippens, H. Steen, et al., Post-translational modification: nature's escape from genetic imprisonment and the basis for dynamic information encoding, Wiley Interdiscip. Rev. Syst. Biol. Med. 4 (6) (2012) 565–583.
[9] L.D. Rogers, C.M. Overall, Proteolytic post-translational modification of proteins: proteomic tools and methodology, Mol. Cell. Proteomics 12 (12) (2013) 3532–3542.
[10] C. Choudhary, B.T. Weinert, Y. Nishida, et al., The growing landscape of lysine acetylation links metabolism and cell signalling, Nat. Rev. Mol. Cell Biol. 15 (8) (2014) 536–550.
[11] M. Arif, B.R. Selvi, T.K. Kundu, Lysine acetylation: the tale of a modification from transcription regulation to metabolism, Chembiochem 11 (11) (2010) 1501–1504.
[12] S. Zhao, W. Xu, W. Jiang, et al., Regulation of cellular metabolism by protein lysine acetylation, Science 327 (5968) (2010) 1000–1004.
[13] C. Choudhary, C. Kumar, F. Gnad, et al., Lysine acetylation targets protein complexes and co-regulates major cellular functions, Science 325 (5942) (2009) 834–840.
[14] G. Liao, L. Xie, X. Li, et al., Unexpected extensive lysine acetylation in the trump-card antibiotic producer Streptomyces roseosporus revealed by proteome-wide profiling, J. Proteome 106 (2014) 260–269.
[15] B.J. Yu, J.A. Kim, J.H. Moon, et al., The diversity of lysine-acetylated proteins in *Escherichia coli*, J. Microbiol. Biotechnol. 18 (9) (2008) 1529–1536.
[16] B.T. Weinert, V. Iesmantavicius, S.A. Wagner, et al., Acetyl-phosphate is a critical determinant of lysine acetylation in *E. coli*, Mol. Cell 51 (2) (2013) 265–272.
[17] M.L. Kuhn, B. Zemaitaitis, L.I. Hu, et al., Structural, kinetic and proteomic characterization of acetyl phosphate-dependent bacterial protein acetylation, PLoS ONE 9 (4) (2014) e94816.
[18] B. Schilling, D. Christensen, R. Davis, et al., Protein acetylation dynamics in response to carbon overflow in *Escherichia coli*, Mol. Microbiol. 98 (5) (2015) 847–863.
[19] K. Zhang, S. Zheng, J.S. Yang, et al., Comprehensive profiling of protein lysine acetylation in *Escherichia coli*, J. Proteome Res. 12 (2) (2013) 844–851.
[20] J. Zhang, R. Sprung, J. Pei, et al., Lysine acetylation is a highly abundant and evolutionarily conserved modification in *Escherichia coli*, Mol. Cell. Proteomics 8 (2) (2009) 215–225.
[21] J. Ren, Y. Sang, J. Ni, et al., Acetylation regulates survival of *Salmonella enterica* serovar Typhimurium under acid stress, Appl. Environ. Microbiol. 81 (17) (2015) 5675–5682.
[22] Y. Sang, J. Ren, J. Ni, et al., Protein acetylation is involved in Salmonella enterica serovar Typhimurium virulence, J. Infect. Dis. (2016).
[23] Q. Wang, Y. Zhang, C. Yang, et al., Acetylation of metabolic enzymes coordinates carbon source utilization and metabolic flux, Science 327 (5968) (2010) 1004–1007.
[24] X. Wu, A. Vellaichamy, D. Wang, et al., Differential lysine acetylation profiles of Erwinia amylovora strains revealed by proteomics, J. Proteome 79 (2013) 60–71.
[25] H. Okanishi, K. Kim, R. Masui, et al., Acetylome with structural mapping reveals the significance of lysine acetylation in Thermus thermophilus, J. Proteome Res. 12 (9) (2013) 3952–3968.
[26] D. Kim, B.J. Yu, J.A. Kim, et al., The acetylproteome of gram-positive model bacterium Bacillus subtilis, Proteomics 13 (10–11) (2013) 1726–1736.
[27] D.W. Lee, D. Kim, Y.J. Lee, et al., Proteomic analysis of acetylation in thermophilic Geobacillus kaustophilus, Proteomics 13 (15) (2013) 2278–2282.
[28] L. Liu, G. Wang, L. Song, et al., Acetylome analysis reveals the involvement of lysine acetylation in biosynthesis of antibiotics in Bacillus amyloliquefaciens, Sci. Report. 6 (20108) (2016) 20108.
[29] Z. Zhang, M. Tan, Z. Xie, et al., Identification of lysine succinylation as a new post-translational modification, Nat. Chem. Biol. 7 (1) (2011) 58–63.
[30] G. Colak, Z. Xie, A.Y. Zhu, et al., Identification of lysine succinylation substrates and the succinylation regulatory enzyme CobB in *Escherichia coli*, Mol. Cell. Proteomics **12** (12) (2013) 3509–3520.
[31] M. Yang, Y. Wang, Y. Chen, et al., Succinylome analysis reveals the involvement of lysine succinylation in metabolism in pathogenic mycobacterium tuberculosis, Mol. Cell. Proteomics **14** (4) (2015) 796–811.
[32] S. Kosono, M. Tamura, S. Suzuki, et al., Changes in the acetylome and Succinylome of Bacillus subtilis in response to carbon source, PLoS ONE 10 (6) (2015) e0131169.
[33] L. Xie, G. Wang, Z. Yu, et al., Proteome-wide lysine glutarylation profiling of the mycobacterium tuberculosis H37Rv, J. Proteome Res. 15 (4) (2016) 1379–1385.
[34] C. Peng, Z. Lu, Z. Xie, et al., The first identification of lysine malonylation substrates and its regulatory enzyme, Mol. Cell. Proteomics 10 (12) (2011) (M111 012658).
[35] J. Park, Y. Chen, D.X. Tishkoff, et al., SIRT5-mediated lysine desuccinylation impacts diverse metabolic pathways, Mol. Cell 50 (6) (2013) 919–930.
[36] Y. Nishida, M.J. Rardin, C. Carrico, et al., SIRT5 regulates both cytosolic and mitochondrial protein malonylation with glycolysis as a major target, Mol. Cell 59 (2) (2015) 321–332.
[37] G. Colak, O. Pougovkina, L. Dai, et al., Proteomic and biochemical studies of lysine malonylation suggest its malonic aciduria-associated regulatory role in mitochondrial function and fatty acid oxidation, Mol. Cell. Proteomics 14 (11) (2015) 3056–3071.
[38] J.-Y. Xu, Z. Xu, Y. Zhou, et al., Lysine malonylome may affect the central metabolism and erythromycin biosynthesis pathway in Saccharopolyspora erythraea, J. Proteome Res. 15 (5) (2016) 1688–1701.
[39] L. Qian, L. Nie, M. Chen, et al., Global profiling of protein lysine malonylation in *Escherichia coli* reveals its role in energy metabolism, J. Proteome Res. (2016).
[40] Z. Liu, A. Budiharjo, P. Wang, et al., The highly modified microcin peptide plantazolicin is associated with nematicidal activity of Bacillus amyloliquefaciens FZB42, Appl. Microbiol. Biotechnol. 97 (23) (2013) 10081–10090.
[41] X.H. Chen, R. Scholz, M. Borriss, et al., Difficidin and bacilysin produced by plant-associated *Bacillus amyloliquefaciens* are efficient in controlling fire blight disease, J. Biotechnol. 140 (1–2) (2009) 38–44.
[42] L. Wu, H. Wu, L. Chen, et al., Difficidin and bacilysin from Bacillus amyloliquefaciens FZB42 have antibacterial activity against Xanthomonas oryzae rice pathogens, Sci. Report. 5 (2015) 12975.
[43] Y. Du, T. Cai, T. Li, et al., Lysine malonylation is elevated in type 2 diabetic mouse models and enriched in metabolic associated proteins, Mol. Cell. Proteomics 14 (1) (2015) 227–236.
[44] A. Koumoutsi, X.H. Chen, A. Henne, et al., Structural and functional characterization of gene clusters directing nonribosomal synthesis of bioactive cyclic lipopeptides in *Bacillus amyloliquefaciens* strain FZB42, J. Bacteriol. 186 (4) (2004) 1084–1096.
[45] K. Schneider, X.H. Chen, J. Vater, et al., Macrolactin is the polyketide biosynthesis product of the pks2 cluster of *Bacillus amyloliquefaciens* FZB42, J. Nat. Prod. 70 (9) (2007) 1417–1423.
[46] J. Moldenhauer, X.H. Chen, R. Borriss, et al., Biosynthesis of the antibiotic bacillaene, the product of a giant polyketide synthase complex of the trans-AT family, Angew. Chem. Int. Ed. Eng. 46 (43) (2007) 8195–8197.
[47] R.A. Butcher, F.C. Schroeder, M.A. Fischbach, et al., The identification of bacillaene, the product of the PksX megacomplex in Bacillus subtilis, Proc. Natl. Acad. Sci. U. S. A. 104 (5) (2007) 1506–1509.
[48] B. Fan, L.C. Carvalhais, A. Becker, et al., Transcriptomic profiling of Bacillus amyloliquefaciens FZB42 in response to maize root exudates, BMC Microbiol. 12 (2012) 116.
[49] B. Fan, L. Li, Y. Chao, et al., dRNA-Seq reveals genomewide TSSs and noncoding RNAs of plant beneficial rhizobacterium Bacillus amyloliquefaciens FZB42, PLoS ONE 10 (11) (2015) e0142002.

[50] J. Cox, M. Mann, MaxQuant enables high peptide identification rates, individualized ppb-range mass accuracies and proteome-wide protein quantification, Nat. Biotechnol. 26 (12) (2008) 1367–1372.
[51] P. Horton, K.J. Park, T. Obayashi, et al., WoLF PSORT: protein localization predictor, Nucleic Acids Res. 35 (2007) (Web Server issue: W585-7).
[52] D. Schwartz, S.P. Gygi, An iterative statistical approach to the identification of protein phosphorylation motifs from large-scale data sets, Nat. Biotechnol. 23 (11) (2005) 1391–1398.
[53] M.F. Chou, D. Schwartz, Biological sequence motif discovery using motif-x, Curr. Protoc. Bioinformatics (2011) 13.15. 1–13.15. 24.
[54] B. Petersen, T.N. Petersen, P. Andersen, et al., A generic method for assignment of reliability scores applied to solvent accessibility predictions, BMC Struct. Biol. 9 (1) (2009) 1–10.
[55] Ben Fan, Li, Y.-L., Lei Li, et al., Malonylome of the plant growth promoting 10 rhizobacterium with potent biocontrol activity, *Bacillus amyloliquefaciens* FZB42. (11 Data in Brief. submitted).
[56] I. Moszer, L.M. Jones, S. Moreira, et al., SubtiList: the reference database for the *Bacillus subtilis* genome, Nucleic Acids Res. 30 (1) (2002) 62–65.
[57] Y. Cao, J. Wu, Q. Liu, et al., sRNATarBase: a comprehensive database of bacterial sRNA targets verified by experiments, RNA 16 (11) (2010) 2051–2057.
[58] M.J. Rardin, J.C. Newman, J.M. Held, et al., Label-free quantitative proteomics of the lysine acetylome in mitochondria identifies substrates of SIRT3 in metabolic pathways, Proc. Natl. Acad. Sci. U. S. A. 110 (16) (2013) 6601–6606.
[59] W. Liang, A. Malhotra, M.P. Deutscher, Acetylation regulates the stability of a bacterial protein: growth stage-dependent modification of RNase R, Mol. Cell 44 (1) (2011) 160–166.
[60] C.T. Walsh, Polyketide and nonribosomal peptide antibiotics: modularity and versatility, Science 303 (5665) (2004) 1805–1810.
[61] X.H. Chen, A. Koumoutsi, R. Scholz, et al., Genome analysis of *Bacillus amyloliquefaciens* FZB42 reveals its potential for biocontrol of plant pathogens, J. Biotechnol. 140 (1–2) (2009) 27–37.
[62] A. Koumoutsi, X.-H. Chen, J. Vater, et al., DegU and YczE positively regulate the synthesis of Bacillomycin D by Bacillus amyloliquefaciens strain FZB42, Appl. Environ. Microbiol. 73 (21) (2007) 6953–6964.
[63] T. Stein, J. Vater, V. Kruft, et al., The multiple carrier model of nonribosomal peptide biosynthesis at modular multienzymatic templates, J. Biol. Chem. 271 (26) (1996) 15428–15435.
[64] A.M. Haapalainen, G. Merilainen, R.K. Wierenga, The thiolase superfamily: condensing enzymes with diverse reaction specificities, Trends Biochem. Sci. 31 (1) (2006) 64–71.
[65] Z. Xie, J. Dai, L. Dai, et al., Lysine succinylation and lysine malonylation in histones, Mol. Cell. Proteomics 11 (5) (2010) 100–107.
[66] E.E. Idris, D.J. Iglesias, M. Talon, et al., Tryptophan-dependent production of indole-3-acetic acid (IAA) affects level of plant growth promotion by *Bacillus amyloliquefaciens* FZB42, Mol. Plant-Microbe Interact. 20 (6) (2007) 619–626.
[67] X. Zhao, Y. Wang, Q. Shang, et al., Collagen-like proteins (ClpA, ClpB, ClpC, and ClpD) are required for biofilm formation and adhesion to plant roots by Bacillus amyloliquefaciens FZB42, PLoS ONE 10 (2) (2015) e0117414.
[68] S.S. Branda, J.E. Gonzalez-Pastor, E. Dervyn, et al., Genes involved in formation of structured multicellular communities by *Bacillus subtilis*, J. Bacteriol. 186 (12) (2004) 3970–3979.
[69] D.B. Kearns, F. Chu, S.S. Branda, et al., A master regulator for biofilm formation by *Bacillus subtilis*, Mol. Microbiol. 55 (3) (2005) 739–749.
[70] E. Lombardia, A.J. Rovetto, A.L. Arabolaza, et al., A LuxS-dependent cell-to-cell language regulates social behavior and development in *Bacillus subtilis*, J. Bacteriol. 188 (12) (2006) 4442–4452.
[71] Z. Huang, G. Meric, Z. Liu, et al., luxS-based quorum-sensing signaling affects biofilm formation in *Streptococcus* mutans, J. Mol. Microbiol. Biotechnol. 17 (1) (2009) 12–19.
[72] C.M. Ryu, M.A. Farag, C.H. Hu, et al., Bacterial volatiles promote growth in Arabidopsis, Proc. Natl. Acad. Sci. U. S. A. 100 (8) (2003) 4927–4932.
[73] T. Rudrappa, M.L. Biedrzycki, S.G. Kunjeti, et al., The rhizobacterial elicitor acetoin induces systemic resistance in *Arabidopsis thaliana*, Commun. Integr. Biol. 3 (2) (2010) 130–138.
[74] F. Gutiérrez-Luna, J. López-Bucio, J. Altamirano-Hernández, et al., Plant growth-promoting rhizobacteria modulate root-system architecture in *Arabidopsis thaliana* through volatile organic compound emission, Symbiosis 51 (1) (2010) 75–83.
[75] R. Ortiz-Castro, H.A. Contreras-Cornejo, L. Macias-Rodriguez, et al., The role of microbial signals in plant growth and development, Plant Signal. Behav. 4 (8) (2009) 701–712.
[76] K.E. van Straaten, H. Zheng, D.R. Palmer, et al., Structural investigation of myo-inositol dehydrogenase from Bacillus subtilis: implications for catalytic mechanism and inositol dehydrogenase subfamily classification, Biochem. J. 432 (2) (2010) 237–247.
[77] M.T. Hilgers, M.L. Ludwig, Crystal structure of the quorum-sensing protein LuxS reveals a catalytic metal site, Proc. Natl. Acad. Sci. U. S. A. 98 (20) (2001) 11169–11174.
[78] Y. Li, Y. Hu, X. Zhang, et al., Conformational fluctuations coupled to the thiol-disulfide transfer between thioredoxin and arsenate reductase in Bacillus subtilis, J. Biol. Chem. 282 (15) (2007) 11078–11083.
[79] J.M. Van Noort, B. Kraal, L. Bosch, et al., Cross-linking of tRNA at two different sites of the elongation factor Tu, Proc. Natl. Acad. Sci. U. S. A. 81 (13) (1984) 3969–3972.
[80] M. Kjeldgaard, J. Nyborg, Refined structure of elongation factor EF-Tu from *Escherichia coli*, J. Mol. Biol. 223 (3) (1992) 721–742.
[81] H. Berchtold, L. Reshetnikova, C.O.A. Reiser, et al., Crystal structure of active elongation factor Tu reveals major domain rearrangements, Nature 365 (6442) (1993) 126–132.
[82] M. Kjeldgaard, P. Nissen, S. Thirup, et al., The crystal structure of elongation factor EF-Tu from Thermus aquaticus in the GTP conformation, Structure **1** (1) (1993) 35–50.
[83] M.J. LaMarche, J.A. Leeds, A. Amaral, et al., Discovery of LFF571: an investigational agent for Clostridium difficile infection, J. Med. Chem. 55 (5) (2012) 2376–2387.
[84] M.J. LaMarche, J.A. Leeds, K. Amaral, et al., Antibacterial optimization of 4-aminothiazolyl analogues of the natural product GE2270 A: identification of the cycloalkylcarboxylic acids, J. Med. Chem. 54 (23) (2011) 8099–8109.
[85] M.J. LaMarche, J.A. Leeds, J. Dzink-Fox, et al., Antibiotic optimization and chemical structure stabilization of thiomuracin A, J. Med. Chem. 55 (15) (2012) 6934–6941.
[86] A. AbouElfetouh, M.L. Kuhn, L.I. Hu, et al., The *E. coli* sirtuin CobB shows no preference for enzymatic and nonenzymatic lysine acetylation substrate sites, Microbiol. Open 4 (1) (2015) 66–83.